ISIJ International, Vol. 49 (2009), No. 10, pp. 1601–1609

Evaluation of the Crystallographic Orientation Relationships between FCC and BCC Phases in TRIP Steels

Kim Verbeken[1,2] Liesbeth BARBÉ[1] and Dierk RAABE[2]

1) Department of Materials Science and Engineering, Ghent University, Technologiepark 903, B-9052 Gent (Zwijnaarde), Belgium. E-mail: kim.verbeken@UGent.be 2) Department of Microstructure Physics and Metal Forming, Max-Planck-Institute for Iron Research, Max-Planck-Strasse 1, Düsseldorf 40237, Germany.

(*Received on April 1, 2009; accepted on May 26, 2009*)

The crystallographic orientation relationships that are active during the transformation of austenite to bainite are studied for two TRIP steels by means of Electron BackScatter Diffraction (EBSD). A detailed evaluation of about 360 retained austenite grains and their BCC neighbours was performed. Three relationships were considered, namely Kurdjumov–Sachs, Nishiyama–Wassermann and Pitsch. It was found that the majority of the austenite grains had at least one neighbour that could be related with one of the three orientation relationships. The Kurdjumov–Sachs relationship appeared to be dominant and no strong indication for variant selection could be retrieved from the studied data. It was, however, also demonstrated that some precautions need to be made since a clear distinction between the evaluation of a small region of the microstructure and conclusions made for the complete material is necessary.

KEY WORDS: TRIP steels; EBSD; phase transformation; crystallographic orientation relationships.

1. Introduction

Cold rolled TRIP steels are subjected to a two-step thermal cycle; an intercritical annealing that aims for a 50% ferrite–50% austenite microstructure followed by an isothermal holding treatment during which the austenite partly transforms to bainite. The crystallography of this type of transformations has already been studied extensively in the literature and different crystallographic orientation relationships have been reported for the transformation of austenite into ferrite, bainite or martensite.[1–6] An overview of these different crystallographic orientation relationships is given in **Table 1**. In this table, the orientation relationships are described by giving the corresponding crystallographic plane and direction in the two phases. For example for the Kurdjumov–Sachs (KS) relationship a $\{111\}_\gamma$ plane is parallel with a $\{110\}_\alpha$ plane and one $\langle 110\rangle_\gamma$ direction lying in this $\{111\}_\gamma$ plane is parallel with a $\langle 111\rangle_\alpha$ direction lying in the corresponding $\{110\}_\alpha$ plane. This orientation relationship is schematically illustrated in **Fig. 1**. The other orientation relationships can be described in a similar manner. An important difference needs, however, to be noted between, on the one hand, the KS, Nishiyama–Wassermann (NW) and Pitsch relationship and, on the other hand, the Greninger–Troiano (GT) and GT′ orientation relationship. While the KS, NW and Pitsch are rational orientation relationships, GT and GT′ are irrational. The difference between these two types of orientation relationships was nicely summarised by Zhang and Weatherly.[7] These authors stated that "the crystallography is rational when an accurate orientation relationship or faceted interfaces can be expressed using a low index $\{hkl\}\langle uvw\rangle$ representation in either crystal base; otherwise it is irrational." Consequently, the values given in Table 1 for GT and GT′ are approximate ones. Numerous research works have been published on irrational orientation relationships (*e.g.* Refs. 8,9)).

Table 1 also gives the number of variants for each orientation relationship. In case of the KS relationship, there are four different $\{111\}_\gamma$ planes, each plane being parallel to a $\{110\}_\alpha$ plane. A $\{111\}_\gamma$ plane contains three different $\langle 110\rangle_\gamma$ directions and each $\langle 110\rangle_\gamma$ direction can be parallel to two different $\langle 111\rangle_\alpha$ directions. Therefore, there are 24 different

Table 1. Overview of the different orientation relationships between face centred and body centred crystals.

Name	Orientation relationship	Number of variants	<uvw>ω_{min}
Bain (B) [1]	$\{100\}_\gamma$// $\{100\}_\alpha$ <100>$_\gamma$// <110>$_\alpha$	3	<1 0 0>45
Kurdjumov-Sachs (KS) [2]	$\{111\}_\gamma$// $\{110\}_\alpha$ <110>$_\gamma$// <111>$_\alpha$	24	<0.97 0.18 0.18> 42.85
Nishiyama-Wasserman (NW) [3, 4]	$\{111\}_\gamma$// $\{110\}_\alpha$ <112>$_\gamma$// <110>$_\alpha$	12	<0.98 0.08 0.20> 45.98
Pitsch (P) [5]	$\{100\}_\gamma$// $\{110\}_\alpha$ <110>$_\gamma$// <111>$_\alpha$	12	<0.08 0.20 0.98> 45.98
Greninger-Troiano (GT) [6]	$\{111\}_\gamma$// $\{110\}_\alpha$ <123>$_\gamma$// <133>$_\alpha$	24	<0.97 0.19 0.13> 44.23
Greninger-Troiano' (GT') [6]	$\{110\}_\gamma$// $\{111\}_\alpha$ <133>$_\gamma$// <123>$_\alpha$	24	<0.19 0.97 0.13> 44.23

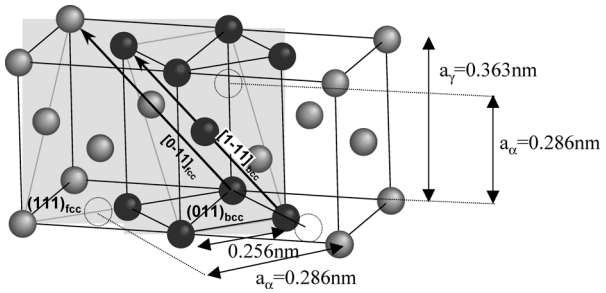

Fig. 1. Schematic illustration of the Kurdjumov–Sachs (KS) orientation relationship.

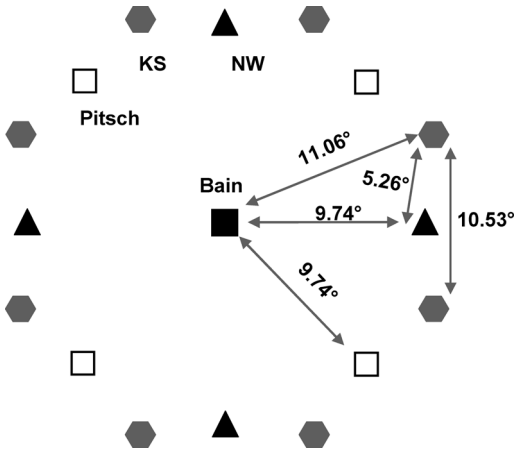

Fig. 2. Schematic overview of all the variants of the KS, NW and Pitsch relationships as how they would appear around one Bain variant on a $\{100\}_{BCC}$ pole figure. The misorientation between these relations together with an explanation of the different symbols is given on the figure.

KS variants. The number of variants for the other orientation relationships can be deduced in a similar way.

A γ–α orientation relationship actually represents a misorientation between two crystallographic orientations. Therefore, this misorientation is most frequently described by means of an axis/angle pair $\langle \mathbf{d} \rangle \omega$. Consequently, the last column of Table 1 gives the axis/angle representation with the minimum misorientation angle of the different orientation relationships.

The Bain orientation relationship is the simplest orientation relationship, but it is never observed in steels. Therefore, this orientation relationship serves as a first approximation or a reference point when the transformation of austenite into a BCC phase is studied. Mostly, the Kurdjumov–Sachs and the Nishiyama–Wassermann relationships are used when the orientation relations between FCC and BCC phases are studied. Although there has been a lot of recent research[10–19] concerning which of these orientation relationships prevails, there is still considerable debate on the relative importance of these orientation relationships because the angular differences between the different orientation relationships is small which makes the experimental verification difficult. Recently, also other orientation relationships[5,6] were taken into account during the study of the crystallographic aspects of the FCC–BCC phase transformation.[10,20] An overview of some features of the different rational orientation relations is given in **Fig. 2**.

Figure 2 illustrates how the different variants of the different orientation relationships would appear around one Bain variant on a $\{100\}_{BCC}$ pole figure. When the three Bain variants are shown on a pole figure, each of them is surrounded by eight KS and four NW variants, respectively. The crystallographic misorientation between two neighbouring KS variants is 10.53°, whilst the misorientation between Bain and a KS variant is 11.06° and the misorientation between Bain and a NW variant is 9.74°. It is shown on Fig. 2 that the four NW variants occupy places in the middle between two KS variants. Consequently, the misorientation between the NW variant and the two surrounding KS variants is 5.26°. The four remaining spots between two KS variants are taken by four variants of the Pitsch orientation relation. Although the corresponding crystallographic planes and directions are different when the Pitsch and NW orientation relation are compared, it can be seen from Table 1 that there is a remarkable resemblance between the two orientation relationships when the axis/angle representation is considered. Moreover, the minimum misorientation angle is exactly the same and the different components of the misorientation axis are only permuted in a different order. Consequently, the distribution of the variants of this orientation relationship around a Bain variant is similar to the one for the NW variants and Pitsch is also called "inverse NW". The Pitsch orientation relationship is mostly related to precipitation in cubic systems, such as Cr-rich precipitates in a Cu–Cr alloy[21] or in a Ni–Cr alloy,[22] α-Fe precipitates in a Cu matrix,[23] γ'-Fe_4N (FCC) precipitates formed in a Fe-matrix (BCC)[24] and cementite/austenite in high carbon steel.[25] Because of the irrational character of the Greninger–Troiano (GT) and GT′ orientation relationships, they are not displayed in Fig. 2, as can be seen from Table 1 and similar to the Pitsch orientation relationship being called "inverse NW", GT′ is also the "inverse GT".

In this work, the γ–α orientation relationships in two phosphorus added TRIP steels are studied with respect to these orientation relationships. Despite the relatively low volume fraction of austenite and the well-known fact that ferrite nucleates with an orientation relationship with respect to the austenite grain and grows inside the neighbouring austenite grains,[26] this material has already been frequently studied in terms of orientation relationships.[11,13,15,16] The present study was performed by means of Electron BackScatter Diffraction (EBSD). Since the development of hardware and software for the automated indexing of EBSD patterns, nearly 15 years ago,[27] this technique has proven to be a very accurate and reliable tool for quantitative microstructural characterisation and can be employed for monitoring the formation of oriented microstructures during evolving processes. By using this technique to evaluate the orientation relationships between the retained austenite grain and its BCC neighbours for a large number of grains, statistically relevant observations for the material as a whole were obtained, which could subsequently be compared with the microstructural details found from examining each retained austenite grain and its neighbours separately.

The studied γ–α orientation relationships are evaluated in terms of the rational KS, NW and Pitsch relationships, since these are the most commonly mentioned and observed in literature. Moreover, the small misorientations be-

tween these orientation relationships and the GT orientation relationships and the irrational character of the latter make it difficult to distinguish between the different orientation relationships. Moreover, the small misorientations that arise during EBSD measurements due to the imperfect fit between the measured and the indexed diffraction pattern also has its effect.

2. Experimental

The EBSD measurements were performed on two different TRIP steels. TRIP1 (0.26 wt% C, 1.62 wt% Mn, 0.51 wt% Si, 0.08 wt% Al, 0.07 wt% P), a Si TRIP steel with no Al additions, was annealed at 785°C for 120 s in a salt bath and austempered at 425°C for 240 s in a second salt bath and subsequently air cooled. The composition of the TRIP2 steel (0.24 wt% C, 1.66 wt% Mn, 0.42 wt% Si, 0.58 wt% Al, 0.07 wt% P) was similar to the previous one except for the addition of Al. This material was annealed at 800°C for 120 s in a salt bath and austempered at 425°C for 240 s in a second salt bath and subsequently air cooled. Phosphorus added TRIP steels make it possible to produce TRIP steels with a high strength combined with good formability. At the same time, these steel grades have several advantages compared with Si and Al TRIP steels. In first instance, these alloys offer good galvanizing properties, which makes them very interesting for the automotive industry. Secondly, they offer an improved weldability, due to their lower carbon content. Details on the effect of the addition of phosphorus on the mechanical properties[28,29] and textures of the different phases[28,30] of low alloyed TRIP steels can be found elsewhere.

The cold rolled and annealed samples of both materials were slowly mechanically polished without electrolytic etching was done. The EBSD measurements were carried out on the plane parallel to the rolling and normal direction. Scans with step sizes between 0.05 and 0.20 μm were carried out on an ESEM equipped with a LaB_6-filament. At first, the materials were scanned for regions with a considerable amount of retained austenite. Subsequently, these regions were scanned in greater detail using a step size of only 0.05 μm. The step size was taken this small because of the fact that the retained austenite islands were small (diameter ~0.5 to 1.5 μm). A greater step size would give rise to only very few data points for each retained austenite grain and would risk eliminating the grain when performing data clean-up procedures. In a standard clean-up procedure, the effect of applying a minimum grain size of three data pixels was examined, but showed not to have a significant influence on the results obtained.

Figure 3 shows an Image Quality (IQ) map of a small region on which a detailed scan was performed. It should be noted that this image does reflect the quality of the diffraction patterns and not the topological features of an etched surface as *e.g.* in optical microscopy or SEM image. A phase map of the same region is shown in **Fig. 4**. On this figure, all grain boundaries (ω>5°) are marked in black. The retained austenite is coloured in red; the different BCC phases are white. Remark the relative absence of grain boundaries within the retained austenite islands. Multiple detail measurements were carried out on both materials in order to be able to improve the statistics of the studied data that were obtained from the measurement. The TRIP1 steel, in particular, required many measurements, because of the lower fraction of retained austenite in this material. The crystallographic features of 194 retained austenite grains and all its neighbours for the TRIP2 material and 173 grains for the TRIP1 material were studied by collecting the crystallographic orientations of each retained austenite grain and all its neighbours.

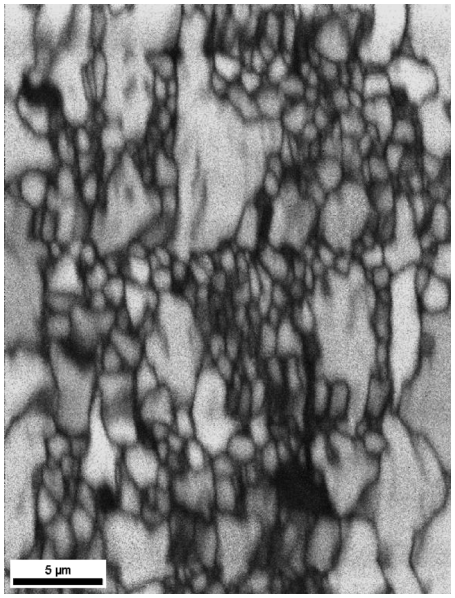

Fig. 3. Image Quality map of a selected region of the TRIP2 steel.

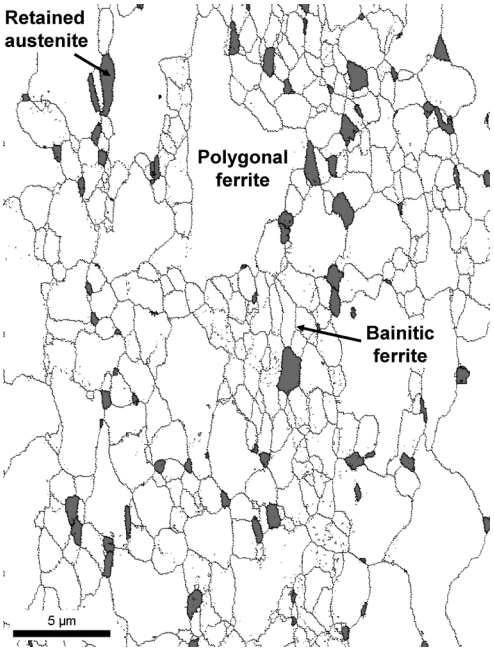

Fig. 4. Phase map of the same region as Fig. 3. All grain boundaries (ω>5°) are in black. Retained austenite is in red, BCC phases in white.

3. Data Analysis Procedure

In this section, a detailed description of the treatment of the data is given in order to clarify the procedure used. At

first, when the results of an OIM measurement are analysed, the orientation data of a specific grain can be extracted with the TSL-OIM software, after manual inspection of the data obtained and excluding those points with a Confidence Index (CI) of less than 0.1. In the software, a point-to-point misorientation of 2° was considered to be the minimal misorientation for a grain boundary.

In the case of a fully recrystallized material, all the data points confined to that specific grain represent, within the limits of error, one identical crystallographic orientation. One arbitrary data point from the bulk of the grain may, in theory, be considered as an acceptable approximation of the average crystallographic orientation of this grain. In practice, however, there will be a spread caused by errors of a stochastic nature. Therefore, it will be more accurate to calculate the average crystallographic orientation and to use this in further calculations.

In order to evaluate the orientation spread within a grain around its average orientation g_{avg}, the Grain Orientation Spread (GOS) parameter, as determined by the TSL-OIM software, is used. This parameter is already used elsewhere to distinguish deformed from recrystallized grains in both steels[31] and aluminium alloys[32,33] with the deformed grains self-evidently showing the larger GOS value because of the strain heterogeneities present.[34] The calculation of the GOS is done by determining the average deviation between the orientation of each individual pixel and the average orientation of the grain. It was found in the present work that GOS values were obtained well below 1° for all grains measured.

Another feature that needs to be dealt with is the fact that in case of cubic crystal symmetry, each crystallographic orientation can be described in 24 different symmetrically equivalent ways. In order to exclude an effect of the arbitrary choice of the EBSD software, a unique representation of each grain average orientation needs to be determined. This was done by limiting Euler space to the most fundamental zone where there is a one–one relation between each possible position of the cubic crystal and the corresponding set of Euler angles.[35]

In order to study the orientation relationships between the parent austenite grain and the daughter bcc grains misorientations need to be calculated. In general, misorientations are described in terms of a rotation axis **d** and a rotation angle ω.[35–37] This notation is often called the axis/angle representation. The rotation axis **d** corresponds to a crystallographic direction common to both neighbouring crystal lattices. The angle ω defines the rotation around the axis **d** which must be applied in order to bring the first crystal into coincidence with the second one. By convention, the smallest misorientation angle ω_{min} and the corresponding misorientation axis are selected to obtain a unique representation of an arbitrarily given misorientation. However, as was already done in previous work,[10,38] misorientations between the parent austenite and the daughter BCC grain were calculated by making use of Rodrigues–Frank vectors. Frank[39] and others[40–44] have argued in favour of the Rodrigues vector representation,[45,46] because this representation offers an intuitively simple space which enables visualisation of the geometric configuration of orientations and misorientations. The Rodrigues–Frank vector **R** is defined by:

$$\mathbf{R} = \mathbf{d} \cdot \tan \frac{\omega}{2}$$

Subsequently, the misorientations between the retained austenite grain and all its neighbours were evaluated for the presence of Kurdjumov–Sachs, Nishiyama–Wassermann or Pitsch orientation relationships. In order to do this evaluation, misorientations were calculated between the crystallographic orientation of the BCC neighbours and those of all the ideal KS, NW and Pitsch variants. The used algorithm provided for each neighbouring grain which orientation relationship and which variant of this orientation relationship matched best the actual BCC crystallographic orientation and also the misorientation between this best fitting variant and the BCC orientation. In order to define the different possible KS, NW or Pitsch variants, the same convention of nomenclature was used as in other work,[10,13] *i.e.* the Bishop and Hill nomenclature[47,48] is used for the KS variants. According to this notation, a, b, c and d correspond to the following planes: (111), $(\bar{1}\bar{1}1)$, $(\bar{1}11)$ and $(1\bar{1}1)$, respectively, and I, II and III refer to the $\langle 01\bar{1}\rangle$, $\langle 101\rangle$ and $\langle 1\bar{1}0\rangle$ directions, respectively. These output files were studied in detail and provided valuable insight on which orientation relationship governed the phase transformation during the intercritical annealing and overageing processes. At first, these data are studied to see if the retained austenite grain had a BCC neighbour with a crystallographic orientation close to one of the predicted KS, NW and Pitsch transformation products. Secondly, it was analysed which orientation relationship and which variant of this orientation relationship coincided with the predicted orientation relationships. This was done by looking at the best fitting prediction of the average BCC grain orientation.

4. FCC–BCC Orientation Relationships in TRIP Steels

The calculated data were used, at first, to see which of all the neighbouring BCC grains fitted best with one of the predicted KS, NW and Pitsch transformation products of the retained austenite grains. Therefore, from each output file the minimum misorientation angle between this BCC grain and the ideal transformation product was gathered. The frequency distribution of these misorientation angles is plotted for both materials in **Fig. 5** using a 5° interval. Because of the relatively small misorientations between the different possible transformation products, the grains with a

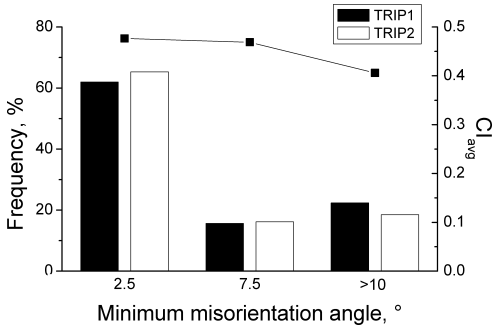

Fig. 5. Misorientation angle distribution for both sets of grains, illustrating the misorientation between a predicted and the best fitting measured BCC grain. The average Confidence Index (CI) of the austenite grains is given as well.

misorientation of more than 10° were grouped in a "$>10°$" interval. It can be seen that for both TRIP steels, almost 2 out of 3 retained austenite grains had at least one neighbouring BCC grain that was within a 5° misorientation of an ideal KS, NW or Pitsch transformation product. When a tolerance angle of 10° is considered, more than 80% of the retained austenite grains had a neighbour close to a predicted transformation product.

This degree of correlation between the actual crystallographic orientation of the BCC grain and the calculated transformation products is of course a good result, but the question why not all the retained austenite grains had a close KS, NW or Pitsch relationship with at least one of its neighbours might be even more challenging. Therefore, a closer look was taken at the features of these remaining retained austenite grains.

At first, the grain average confidence index (CI)* of the data that were gathered from the microtexture analysis software as the representative crystallographic orientation for the BCC and FCC grains was considered. Since the BCC grains, both ferrite and bainite, were large compared with the retained austenite grains, they were easier to measure and consequently their average CI was very high, *i.e.* 0.5 or higher. The retained austenite was, however, more difficult to measure because of the size of the retained austenite islands and the limited SEM resolution, which was due to the use of a LaB_6 rather than a FEG electron source. Therefore, an average confidence index was calculated for all the retained austenite grains within each interval of Fig. 5. This average confidence index is also shown in Fig. 5. It is clear from this graph that the retained austenite grains that did not have a neighbour with a close correlation with an ideal KS, NW or Pitsch transformation product have a lower average CI. While within the first misorientation intervals, the CI of the retained austenite grains was reasonably high, *i.e.* 0.4 or higher, the CI of the retained austenite grains in the other intervals, *i.e.* with a misorientation of more than 10°, appears to be lower.

A second reason, besides the relation with the CI and which certainly has an effect on the features that are deduced from the calculations, is that an EBSD measurement only provides information of one 2D section of a 3D microstructure. Clearly, a retained austenite grain can and will have close-to KS, NW or Pitsch orientation relationships with neighbouring BCC grains in three dimensions, but part of these neighbours will remain undetected in a 2D section.

A third reason is found in the relationship that is observed between the number of neighbouring BCC grains a retained austenite grain has and the interval where this grain appeared in Fig. 5. It was shown that grains that are found in the intervals with the lowest misorientation angle have an average number of neighbours between three and four, while grains in the intervals with the highest misorientation angle have on average between two and three neighbours. A closer inspection of the OIM maps reveals that many of the retained austenite grains from the high angle intervals are surrounded by two polygonal ferrite grains in the measured section and looking at all the output files learned that the polygonal ferrite can rarely be correlated with the retained austenite grains through one of the considered orientation relationships. This last feature is of course a self evident consequence of the partial phase transformation that occurs during the two step annealing cycle to which the studied materials are subjected and the fact that ferrite will grow in the adjacent grain, while bainite grows within the grain in which it nucleated.

5. Evaluation of Variant Selection

After considering which neighbouring BCC grains fitted best with one of the predicted KS, NW and Pitsch transformation products of the retained austenite, these data are investigated in more detail. This detailed study will focus mostly on those retained austenite grains that had a neighbour transformation product with the misorientation angle within the 0–5° interval. A higher tolerance angle might improve the statistics of the results and in studies where it is investigated if a certain misorientation relationship is followed, such as studies on selective growth during recrystallization or when spreads around ideal texture components are applied, often a higher tolerance angle such as 10°[38,49] or 15°,[50–52] the latter one corresponding to the maximum misorientation of a low angle grain boundary, is used. In this case, however, a tolerance angle of 5° was chosen because this tolerance is, as was illustrated in Fig. 2, smaller than the maximum misorientation between a KS and a NW or Pitsch variant, which is 5.26°.

Figure 6 displays a frequency distribution showing which orientation relationship provided the best prediction of the real crystallographic orientations of the best fitting BCC grain that surrounded the retained austenite. This figure shows that the Pitsch orientation relationship is clearly the least dominant orientation relationship. This feature is in good accordance with all literature data, which always suggest a dominance of the KS or NW orientation relationship. In the present study, for both materials, the KS orientation relationship appears to be the more dominant one.

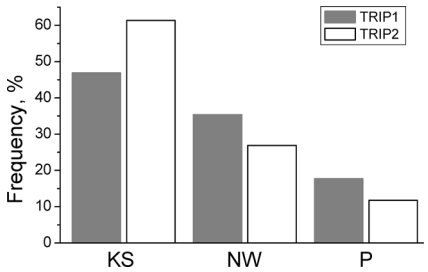

Fig. 6. Histogram showing for both materials which the orientation relationship was between the retained austenite grain and the best fitting measured BCC grain. Only those cases where the misorientation was less than 5° were included.

* The reliability of the indexing of the diffraction pattern by the software is quantified by the confidence index, which ranges from 0 to 1. For a given diffraction pattern severable possible orientations may be found which lead to an acceptable indexing of the diffraction data. The software ranks these orientations using a voting scheme on which basis the CI is calculated. If the first two orientations on the voting scheme have the same amount of votes, a CI of 0 is achieved.

This is in particular the case for TRIP2, where in nearly two out of three cases the KS relationship is observed. These findings should, however, always be stated with the necessary precautions. As will be shown in the next section, several retained austenite grains will display a good correspondence with the ideal KS, NW or Pitsch orientation relationship with several of their BCC neighbours, whilst the conclusions made above were only based on considering the best fitting neighbouring BCC grain. Furthermore, BCC grains might even have a better fitting relation with an austenite grain which is not detectable due to the measurement of a 2D section of a 3D material.

Therefore, macroscopic conclusions on which crystallographic orientation relationship prevails for a complete material should be made with relative care. Although, the relative inaccuracy of about 0.5 to 1.0° in the angular resolution of the experimental technique used, *i.e.* EBSD, and the small misorientations between the different orientation relationships have to be considered, it can be said that in cases of solid–solid transformations, when there is a lack of prestrain or of an external loading, the microscopical 'environment' might play an important role in determining which variant of which orientation relationship governs the transformation of one particular grain. In the present case, during the transformation of the parent austenite grain, the crystallographic orientation of the daughter bainite has to contain possible influences from the microstructural environment of the grain, such as the interaction of the grain with its neighbours, the possible presence of micro-stresses or residual stresses and the accommodation of the transformation strain. Moreover, these factors not only tend to influence the crystallographic orientation of the forming bainite, but could also affect the remaining retained austenite or other neighbouring BCC grains. The above mentioned factors, which act locally in the material, might play a non-negligible role on the choice of the active orientation relation during transformation comparable to the self accommodating variants that are also described for other solid–solid transformations, such as martensitic transformations.[53–55] However, in order to further support the possible influence of the local environment of the transformation process, the present results have to be validated by measurements of internal stresses, for example by neutron diffraction measurements, as was done by Sittner *et al.*[56]

For the sake of completeness, **Table 2** provides an overview on how the relative importance of the different orientation relationships evolves with increasing tolerance angle. In both cases, the dominance of the KS relationship becomes somewhat stronger and the Pitsch orientation relationship clearly remains the least important one. Further on, the data will be studied to see how the distribution between the different variants was for each orientation relationship. Since both TRIP steels show very similar results so far and in order to improve the statistics of the present data, the data of both TRIP steels were gathered when studying the possible occurrence of variant selection.

Figure 7 shows the distribution of the different variants for the KS, NW and Pitsch orientation relationship. The data are the result of 126 KS, 72 NW and 34 Pitsch orientation relationships. These data are studied by taking into account the crystallographic features of the different variants.

Table 2. Overview showing for both materials and for several intervals of misorientation angles which the orientation relationship was between the retained austenite grain and the best fitting measured BCC grain.

	TRIP1			TRIP2		
	0°-5°	0°-10°	0°-15°	0°-5°	0°-10°	0°-15°
KS	47%	48%	52%	61%	62%	66%
NW	35%	36%	32%	27%	24%	21%
P	18%	16%	16%	12%	14%	13%

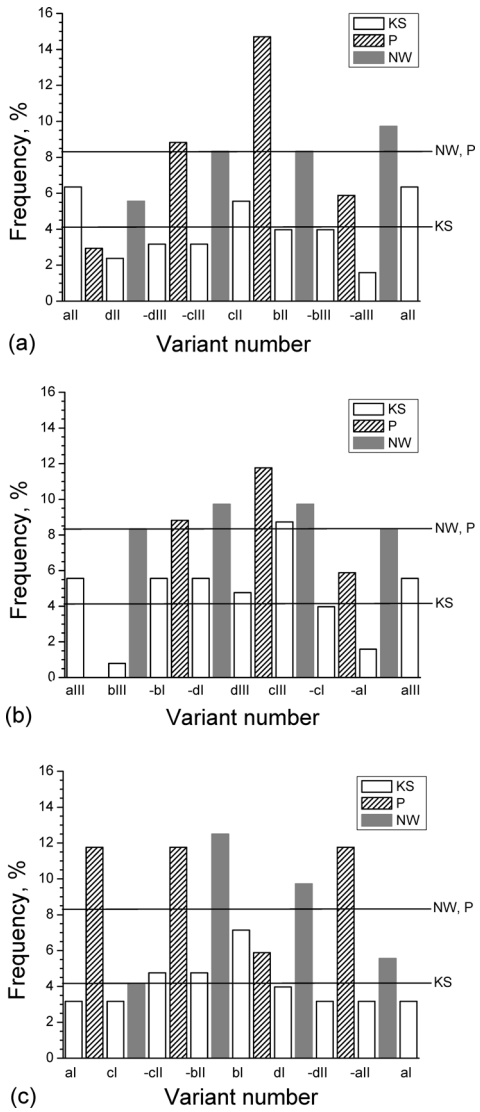

Fig. 7. Distribution of the different variants for the KS, NW and Pitsch orientation relationships, grouped as how they appear around the three Bain variants on a $\{100\}_{BCC}$ pole figure. The horizontal lines indicate the frequency levels in case of no variant selection.

In Fig. 7, the variants are gathered in three groups, similarly as how they appear around the Bain variants on a $\{100\}_{BCC}$ pole figure (*cf.* Fig. 2). The nomenclature of the different variants was explained above. The horizontal lines on Fig. 7 indicate the frequency levels in case of no variant selection.

From Fig. 7, it is clear that for the KS relationship all variants are present in the studied orientation data. Moreover, most variants have a frequency close to what could be expected if there would not be any variant selection. All NW variants are present as well. Here, a distribution that is

even closer to the case without variant selection is found. It should be noted that the data for the NW orientation relationship are statistically better than for the KS or Pitsch relationship since this relationship is 72 times evaluated for 12 possible variants. For the distribution of the Pitsch orientation relationship, one of the variants appears to be missing. This might be due to the smaller amount of measured Pitsch relationships. Despite the somewhat less statistics, most other variants seem to have a frequency close to the value for the case of no variant selection. In summary, it can be stated that all results shown in Fig. 7 give a strong indication towards a lack of macroscopic variant selection. Although this conclusion opposes against indications given in previous work,[16] it could be expected since the absence of variant selection can be related to the lack of prestrain and external loading during the present solid–solid phase transformation. No indications were found that this difference might be related with the fact that this previous work was performed on conventional (Si, Al) TRIP steel, while present work is on P added TRIP steel.

6. Detailed Study of a Few Selected Regions

In this section, four different regions are selected from the detailed OIM measurements that were carried out on the TRIP2 material. These regions illustrate some characteristics of the studied microstructure, from which several examples could be found in the performed measurements. Moreover, the data that will be discussed below are retrieved from a measured region of only 144 μm^2.

Figure 8 shows a retained austenite grain, coloured in red, and two bainitic transformation products of this grain, namely grain 1 and grain 2. These three grains are completely surrounded by a ferritic grain, namely grain 3, which had a diameter of about 10 μm. Low and high angle grain boundaries are depicted in black on this figure. The study of the orientation relationships between the retained austenite and the surrounding BCC grains reveals that the orientation relationship between the austenitic island and the two bainitic grains are both close to a variant of the Kurdjumov–Sachs orientation relationship. The relation between grain 1 and the retained austenite was 2.5° away from a complete match with variant cIII of the KS orientation relationship, while grain 2 appears to show a 5.9° difference with variant —aIII of the same orientation relationship. Although this is certainly not always the case a correlation could be made between the polygonal ferrite and the retained austenite. This polygonal ferrite grain has only a mismatch of 8.9° with yet another variant, *i.e.* variant dIII, of the KS relationship applied on the retained austenite. The analysis of the orientation relationships of this retained austenite grain shows that the active plane was different for the different grains, the direction was, however, the same for the three grains.

Figure 9 shows two retained austenite grains, namely grain A and grain B. These grains display a misorientation of 17.4° with respect to each other, so they must originate from different intercritical austenite grains. Both grains have multiple BCC neighbours; grain A has 5 neighbours and grain B has 6 neighbours. Several of these grains are neighbours of both retained austenite grains, namely grain

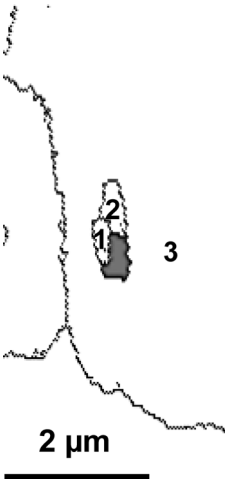

Fig. 8. Retained austenite and some of its transformation products found within one polygonal ferrite grain. The retained austenite grain is in red, BCC grains are in white. All grain boundaries (ω>5°) are in black.

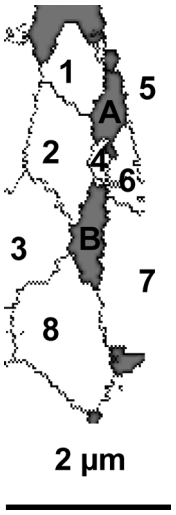

Fig. 9. Two retained austenite grains and their neighbours. The retained austenite grains are in red, BCC grains are in white. All grain boundaries (ω>5°) are in black.

2, 4 and 6. The features of this microstructure and the size of the grains give the indication that grains 1, 2, 4, 6 and 8 are bainitic transformation products that were formed during the second step of the annealing cycle to which the material was subjected. Grains 3, 5 and 7 are most likely polygonal ferrite grains as their diameter is larger than 3 μm. The orientation relationships between the two retained austenite grains and all their neighbours were investigated and the results are shown in **Table 3**. This table gives an overview of the different orientation relationships that are observed. The minimum misorientation angle, together with the active orientation relationship and variant number (*cf.* Fig. 7) are also displayed in Table 3.

From these results it is found that grain A shows a very good correspondence between the different predicted transformation products and almost all its neighbours; 4 out of 5 neighbours have a misorientation of less than 4°. Both the Kurdjumov–Sachs and the Nishiyama–Wassermann orientation relationship appear to apply and different variants are observed. Grain B displays misorientations below 10° with

Table 3. Overview of the observed orientation relationships between two retained austenite grains and all their BCC neighbours. The minimum misorientation angle, together with the active orientation relationship and variant (*cf.* Fig. 7) are given.

FCC grain	BCC grain	Misorientation	Orientation relationship	Variant number
A	**1**	11.2°	KS	-cIII
	2	3.4°	KS	aIII
	4	3.9°	NW	cI(-cII)
	5	1.3°	KS	dII
	6	1.1°	NW	dII(-dIII)
B	**2**	4.2°	KS	bII
	3	1.4°	NW	aIII(-aI)
	4	5.7°	NW	dII(-dIII)
	6	3.2°	Pitsch	-bI(-dI)
	7	7.8°	KS	cII
	8	9.5°	KS	aIII

all its neighbours. Moreover, all three orientation relationships, which are taken into account in this work, are found for this grain. Therefore, it can be deduced from these data that the performed analysis of the active orientation relationship when searching for the dominant orientation relationship, as well as for the occurrence of variant selection, should be treated with the necessary precautions. When considering these results, a similar discussion as in the previous section could be made indicating a possible non-negligible role of the local environment of the transforming grain. Several other examples of a detailed analysis of this type of areas can be found elsewhere.[57)]

7. Conclusions

In the present work, different orientation relationships, *i.e.* the Kurdjumov–Sachs, Nishiyama–Wassermann and Pitsch orientation relationships, were considered to study the features of the transformation of retained austenite to bainite in TRIP steels. Although it was found that there is a dominance of the Kurdjumov–Sachs orientation relationship and that there are no signs of macroscopic variant selection in the studied data, it is also demonstrated that conclusions for the complete material should be drawn with care. Indeed, it was observed that several austenite grains showed a good correspondence with the ideal KS, NW or Pitsch orientation relationship with different BCC neighbours. Moreover, it should be noted that the misorientations between variants of the different orientation relationships are quite small. Therefore, it can be deduced from these data that when searching for the dominant orientation relationship, the influence of the local environment of the grain might have an impact on the phase transformation in "the selection" of a specific orientation relationship or variant.

REFERENCES

1) E. C. Bain: *Trans. AIME*, **70** (1924), 25.
2) G. Kurdjumov and G. Sachs: *Z. Phys.*, **64** (1930), 325.
3) Z. Nishiyama: *Sci. Rep. Inst.*, **23** (1934/1935), 638.
4) G. Wassermann: *Arch. Eisenhüttenwes.*, **16** (1933), 647.
5) W. Pitsch: *Acta Metall.*, **10** (1962), 897.
6) A. B. Greninger and A. R. Troiano: *Trans. AIME*, **140** (1940), 307.
7) W. Z. Zhang and G. C. Weatherly: *Prog. Mater. Sci.*, **50** (2005), 181.
8) J. M. Howe, H. I. Aaronson and J. P. Hirth: *Acta Mater.*, **48** (2000), 3977.
9) J. F. Nie, X. L. Xiao, C. P. Luo and B. C. Muddle: *Micron*, **32** (2001), 857.
10) Y. He, S. Godet and J. J. Jonas: *Acta Mater.*, **53** (2005), 1179.
11) S. Zaefferer, J. Ohlert and W. Bleck: *Acta Mater.*, **52** (2004), 2765.
12) H. J. Bunge, W. Weiss, H. Klein, L. Wcislak, U. Garbe and J. R. Schneider: *J. Appl. Cryst.*, **36** (2003), 137.
13) J. J. Jonas, Y. He and S. Godet: *Scr. Mater.*, **52** (2005), 175.
14) G. Brückner, J. Pospiech, I. Siedl and G. Gottstein: *Scr. Mater*, **44** (2001), 2635.
15) B. Verlinden, Ph. Bocher, E. Girault and E. Aernoudt: *Scr. Mater*, **45** (2001), 909.
16) M. De Meyer, L. Kestens and B. C. De Cooman: *Mater. Sci. Technol.*, **17** (2001), 1353.
17) H. Réglé, N. Maruyama and N. Yoshinaga: Proc. of the Int. Conf. on Advanced High Strength Sheet Steels for Automotive Applications, AIST, Warrendale, PA, (2004), 239.
18) C. Cabus, H. Réglé and B. Bacroix: Proc. of the Int. Conf. on Advanced High Strength Sheet Steels for Automotive Applications, AIST, Warrendale, PA, (2004), 259.
19) D. Raabe: *Acta Mater.*, **45** (1997), 1137.
20) J. J. Jonas, Y. He and S. Godet: *Mater. Sci. Forum*, **495–497** (2005), 1177.
21) M. G. Hall, H. I. Aaronson and K. R. Kinsman: *Surf. Sci.*, **31** (1972), 257.
22) C. P. Luo and G. C. Weatherly: *Acta Metall.*, **35** (1987), 1963.
23) T. Fujii, T. Mori and M. Kato: *Acta Metall. Mater.*, **40** (1992), 3413.
24) U. Dahmen, P. Ferguson and K. H. Westmacott: *Acta Metall.*, **35** (1987), 1037.
25) M. A. Mangan, M. V. Kral and G. Spanos: *Acta Mater.*, **47** (1999), 4263.
26) H. K. D. H. Bhadeshia: *Prog. Mater. Sci.*, **29** (1985), 321.
27) B. L. Adams, S. I. Wright and K. Kunze: *Metall. Trans. A*, **24** (1993), 819.
28) L. Barbé: Physical Metallurgy of P-alloyed TRIP Steels, Doctoral Thesis UGent, ISBN 90-8578-037-3, (2005).
29) L. Barbé, K. Verbeken and E. Wettinck: *ISIJ Int.*, **46** (2006), 1249.
30) K. Verbeken, L. Barbé and B. C. De Cooman: *Mater. Sci. Forum*, **539–543** (2007), 3347.
31) L. Bracke, K. Verbeken, L. Kestens and J. Penning: *Acta Mater.*, **57** (2009), 1512.
32) B. S. El-Dasher, M. H. Alvi and A. D. Rollett: Hot Deformation of Aluminum Alloys III, ed. by T. Bieler, Z. Jin, A. Beaudoin and B. Radhakrishnan, Warrendale, USA, (2003).
33) M. H. Alvi, S. Cheong, H. Weiland and A. D. Rollett: *Mater. Sci. Forum*, **467–470** (2004), 357.
34) K. Verbeken and L. Kestens: *Mater. Sci. Forum*, **408–412** (2002), 559.
35) J. Hansen, J. Pospiech and K. Lücke: Tables for Texture Analysis of Cubic Crystals, Springer, Berlin, (1978).
36) G. Ibe and K. Lücke: *Texture*, **1** (1972), 87.
37) J. Pospiech: *Kristall Tech.*, **7** (1972), 1057.
38) K. Verbeken, L. Kestens and M. D. Nave: *Acta Mater.*, **53** (2005), 2675.
39) F. C. Frank: *Meter. Trans. A*, **19** (1988), 403.
40) R. Becker and S. Panchanadeeswaran: *Textures Microstruct.*, **10** (1989), 167.
41) P. Neumann: *Textures Microstruct.*, **14–17** (1991), 53.
42) P. Neumann: *Phys. Stat. Sol. A*, **131** (1992), 555.

43) V. Randle: Microstructure Determination and Its Applications, London Institute of Mater. Sci., London, (1992).
44) O. Engler, G. Gottstein, J. Pospiech and J. Jura: Proc. 10th Int. Conf. On Textures of Materials, ICOTOM 10, ed. by H.J. Bunge, Trans. Tech. Publications, Switzerland, (1994), 259.
45) L. Euler: *Nov. Comm. Acad. Sci. Imp. Petrop.*, **20** (1775), 208.
46) O. Rodrigues: *J. Mathématique Pures et Appliquées*, **5** (1840), 380.
47) J. F. Bishop and R. Hill: *Philos. Mag.*, **42** (1951), 414.
48) J. F. Bishop and R. Hill: *Philos. Mag.*, **42** (1951), 1298.
49) I. Cross and V. Randle: *Scr. Mater.*, **48** (2003), 1587.
50) K. Verbeken and L. Kestens: *Acta Mater.*, **51** (2003), 1679.
51) C. Cabus, H. Réglé and B. Bacroix: *Mater. Charact.*, **58** (2007), 332.
52) Ph. Gerber, J. Tarasiuk, Th. Chauveau and B. Bacroix: *Acta Mater.*, **51** (2003), 6359.
53) K. Otsuka and X. Ren: *Prog. Mater. Sci.*, **50** (2005), 511.
54) Y. Aydogdu, A. Aydogdu and O. Adiguzel: *J. Mater. Process. Technol.*, **123** (2002), 498.
55) S. Kajiwara: *Metall. Trans. A*, **17A** (1986), 1693.
56) Y. Tomota, S. Harjo, P. Lukas, D. Neov and P. Sittner: *JOM*, **52** (2000), 32.
57) K. Verbeken, L. Barbé, and D. Raabe: *Ceramic Transactions*, **200** (2009), 333.